THE JOURNAL OF PHYSICAL CHEMISTRY C

Article

pubs.acs.org/JPCC

Modeling the Cooperative Energy Transfer Dynamics of Quantum Cutting for Solar Cells

Freddy T. Rabouw and Andries Meijerink*

Condensed Matter and Interfaces, Debye Institute for Nanomaterials Science, Princetonplein 1, 3584 CC Utrecht, The Netherlands

ABSTRACT: Cooperative energy transfer (ET) is a quantum cutting (or downconversion) process where a luminescent center splits its excited state energy in two by simultaneous transfer to two nearby acceptor centers, thus yielding two low-energy photons for each high-energy photon absorbed. It has the potential to greatly enhance the efficiency of phosphors for lighting or the UV/blue response of next generation photovoltaics. Many pairs of luminescent centers have been claimed to enable quantum cutting by cooperative ET. However, direct proof that the ET mechanism is cooperative is often lacking. Here we present a model that can be used to fit or predict the dynamics of cooperative ET in codoped crystals, as a function of the concentration of acceptor centers. It also yields an analytical expression for the efficiency of cooperative ET. Our model can be used to provide evidence for quantum cutting materials, quantify the ET parameter(s), and optimize the doping concentration.

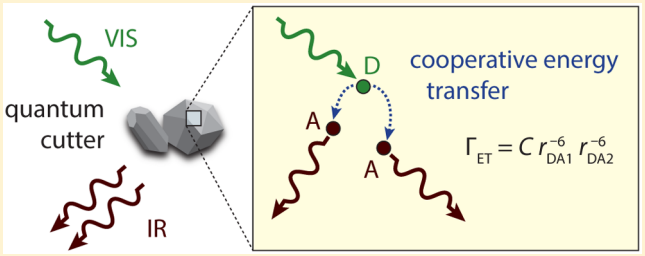

INTRODUCTION

Phosphor materials convert one color of light to another. They are used in devices such fluorescent lamps and LED displays. Many phosphors are microcrystalline materials doped with luminescent ions. It can be desirable to combine different luminescent centers in the same phosphor material. This allows that one of the centers is optimized for strong absorption and transfers its energy to a different type of center, optimized for efficient emission of the desired color of light. Such a scheme also enables easier control over the phosphor properties, e.g., large "Stokes" or "anti-Stokes" shifts important in emerging technologies such as background-free biolabeling[1] or luminescent solar concentrators.[2] Of particular interest are couples of luminescent centers in which "quantum cutting" (or "downconversion") can take place.[3−5] In this process the excitation energy on a donor center is split in two, potentially yielding two emitted photons per absorption event. Splitting occurs either by "cooperative" energy transfer (ET) where the energy is simultaneously transferred to two (or more) nearby acceptor centers[6] or by cross-relaxation where the donor transfers only part of its excitation energy to an acceptor.[7−10] The maximum possible photon-to-photon conversion efficiency of downconversion phosphors is 200%. While the search for downconversion phosphors was initiated by the lighting industry, even more challenging and promising applications are in next-generation photovoltaics. If the wavelength of the emitted downconverted photons can be matched to the bandgap E_g of a solar cell material, a downconversion layer would in principle be able to boost the response of the solar cell to high-energy photons from the solar spectrum ($h\nu > 2E_g$) by a factor of 2.

Many materials have been reported to perform downconversion or quantum cutting.[11,12,14−17] Usually they are doped with lanthanide ions, where the rich energy level structure allows for many different types of ET processes. Often it is straightforward to demonstrate that ET takes place from one type of lanthanide ion to another, by recording emission and excitation spectra.[11−17] The challenge is to actually prove the occurrence of quantum cutting in a particular couple and identify which ET mechanism is operative (e.g., cooperative ET or cross-relaxation). Ideally, an integrating-sphere measurement would demonstrate a quantum efficiency of >100%, i.e., that more photons are emitted than absorbed. However, such direct proof can only be obtained if both the ET and the emission of the downconverted light in the phosphor are very efficient. Any significant loss channel would make the overall quantum efficiency drop below 100%, even if quantum cutting does take place in the material. For example, "space-separated" quantum cutting was demonstrated with an integrating-sphere measurement[18] in closely separated Si nanocrystals. Because the overall quantum efficiency does not exceed 100%, proof of quantum cutting had to come from a stepwise increase of quantum efficiency when the excitation energy was increased to above twice the emission energy. This method is not generally applicable to other quantum cutting materials, unless they have a continuous excitation spectrum.

A more general way to prove quantum cutting, not obscured by efficiency losses due to other processes, is to examine the ET dynamics. Photoluminescence (PL) decay measurements of the donor emission reveal the rate of ET. By investigating how the ET rate changes with increasing acceptor doping concentration in the material, one can establish the type of ET process that takes place. For example, our group has demonstrated that

Received: November 24, 2014
Revised: January 9, 2015
Published: January 16, 2015

DOI: 10.1021/jp511733g
J. Phys. Chem. C 2015, 119, 2364−2370

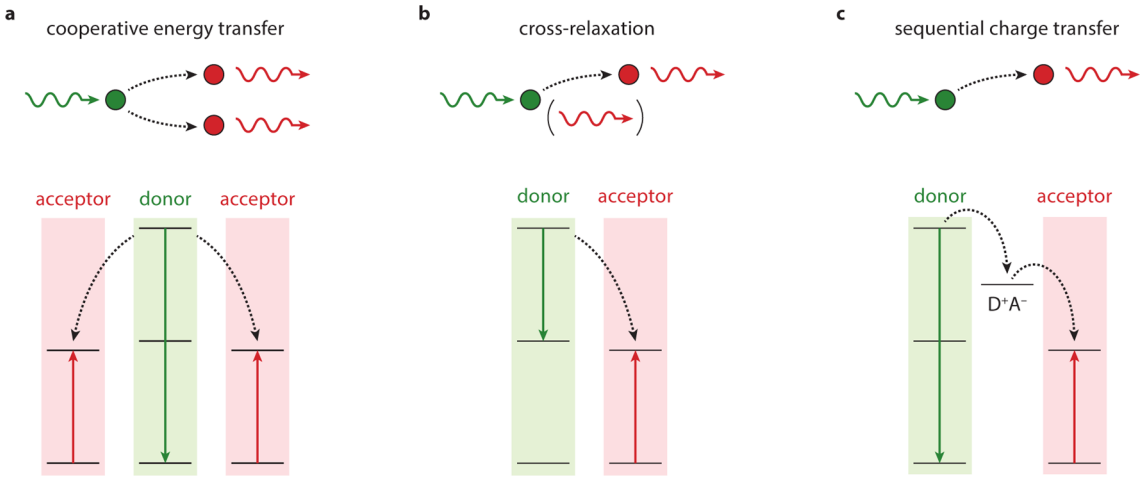

Figure 1. ET mechanisms between lanthanide donor−acceptor pairs. Various ET pathways are possible, in a couple where the donor has a state at energy E and the acceptor a state at energy $E/2$. (a) Cooperative ET is simultaneous transfer to two nearby acceptors. If the acceptor emits efficiently, the result is two emitted photons for one absorbed photon. (b) In the case of cross-relaxation the acceptor transfers only part of its energy to a single acceptor, reaching some intermediate state. This leads to a 1-to-2 photon conversion only if both the acceptor and the intermediate state of the donor emit. (c) Sequential charge transfer can effectively transfer the donor energy to a single acceptor via an intermediate charge transfer state, where all excess energy is lost as heat.

YPO_4:Tb^{3+},Yb^{3+} is a promising downconversion material because ET from Tb^{3+} to Yb^{3+} is cooperative.[6] $LiYF_4$:Pr^{3+},Yb^{3+} also exhibits downconversion, but here the ET process responsible was shown to be cross-relaxation from Pr^{3+} to Yb^{3+}.[9] In contrast, YAG:Ce^{3+},Yb^{3+} is not a good downconversion material because ET from Ce^{3+} to Yb^{3+} is single-step downshifting via an intermediate Ce^{4+}−Yb^{2+} charge transfer state,[13,19] where half of the original energy is lost as heat.

In these previous works a Monte Carlo method was used to model the ET dynamics as a function of acceptor concentration.[6,9,19] By comparing the modeled dynamics to the experimental PL decay curves one can distinguish between different ET mechanisms. For first-order ET processes (i.e., one donor transfers to one acceptor) we have shown that, with the same assumptions as done in the Monte Carlo model (see below), there is an exact analytical expression for the ET dynamics.[9,19,20] In addition, the Inokuti-Hiroyama[21] and Yokota-Tanimoto[22] models provide approximate formulas by neglecting that the crystalline structure of the host material imposes a discrete distribution of donor−acceptor separations. These models are used in many publications to fit ET dynamics and quantify ET rate constants and efficiencies. Unfortunately, a convenient analytical expression for cooperative ET—important for quantum cutting—has not been reported yet.

Here we present a quasi-continuous model for cooperative ET, which yields an analytical approximation for the cooperative ET dynamics and for the cooperative ET efficiency as a function of acceptor concentration. It explicitly takes into account the possible nearest-neighbor configurations of each donor center but averages out the acceptor density beyond the nearest-neighbor shell. The quasi-continuous model very accurately reproduces the results of the more involved Monte Carlo model when applied to the data of Vergeer et al.[6] We further test that the model yields a good approximation of the ET dynamics as well as of the ET efficiency, independent of whether the host crystal geometry has a high or a low symmetry. In the end we briefly discuss that our model can easily be adjusted or extended to include the possibility of (a combination of) other ET mechanisms.

DOWNCONVERSION BY COOPERATIVE ENERGY TRANSFER

Potential downconversion phosphors codoped with luminescent centers must exhibit emission from the acceptor center upon excitation of the donor. However, such observation alone does not prove downconversion. The claim of downconversion by cross-relaxation is often supported by a comparison between excitation spectra of the acceptor luminescence and of the donor luminescence.[7,8,10] While such analysis demonstrates from which energy level on the donor ion transfer to the acceptor occurs, it does not prove which ET mechanism is operative if several are possible. Our group has previously analyzed the ET dynamics in potential downconversion phosphors to investigate the contribution of cooperative ET.[6,9,19] In YPO_4 the ET from Tb^{3+} to Yb^{3+} was found to be cooperative[6] (Figure 1a). Hence, there is true quantum cutting which (depending on the quantum efficiency of Yb^{3+} emission) can yield two NIR photons for each UV/blue excitation. In $LiYF_4$ the ET from Pr^{3+} to Yb^{3+} was shown to be cross-relaxation from ($^3P_0$, $^7F_{7/2}$) to ($^1G_4$, $^7F_{5/2}$)[9] (Figure 1b). Also here the final result can be two NIR photons from Yb^{3+} for each blue excitation because after cross-relaxation the intermediate $^1G_4$ state of Pr^{3+} can transfer its energy to a second Yb^{3+} acceptor center. ET from Ce^{3+} to Yb^{3+} in YAG, on the other hand, can never lead to downconversion with a quantum efficiency of >100% because it is a one-donor-to-one-acceptor process via an intermediate charge transfer state[13,19] (Figure 1c).

The dynamics and efficiency of *first-order* ET processes involving a single acceptor center (such as in Figure 1b,c) can be calculated analytically, under the assumptions that: (1) donor and acceptor centers randomly substitute cation sites in a crystal (justified by the chemical similarity of the lanthanide ions), (2) the ET rate is only dependent on the distance between the donor and acceptor centers (not on the orientation of the transition moments), and (3) no energy

DOI: 10.1021/jp511733g
J. Phys. Chem. C 2015, 119, 2364−2370

migration takes place over the donor sublattice.[9,19,20] Alternatively, there are simpler approximate expressions that ignore the discreteness of the crystal geometry[21] but that can be extended to include the effect of donor-to-donor energy migration.[22] In contrast, the possibility of *second-order* cooperative ET has until now only been analyzed with a Monte Carlo model. Sometimes the continuous models of Inokuti-Hiroyama or Yokota-Tanimoto for *first-order* ET are used, without justification, to fit cooperative ET.[11,14]

Below we first briefly describe how the Monte Carlo model of cooperative ET works. We then show that with an approximation one can obtain an analytical "quasi-continuous" expression for the dynamics and efficiency of cooperative ET. As for the first-order ET processes, both the Monte Carlo and the quasi-continuous model make the basic assumptions that (1) donors and acceptors are randomly distributed over cation sites in the crystal, (2) the ET rate depends only on the distance between donor and acceptors, and (3) there is no donor-to-donor energy migration. The difference with the first-order ET processes is that cooperative ET involves two (rather than one) simultaneous steps: ET from the donor to acceptor A and ET from the same donor to acceptor B. The rate of cooperative ET via dipole−dipole interaction from the donor to the acceptor pair (A,B) is proportional to the inverse sixth power of both donor−acceptor separations

$$\Gamma_{coop} = C_{coop} r_A^{-6} r_B^{-6} \tag{1}$$

where C_{coop} is a constant representing the cooperative ET strength for the particular donor−acceptor couple. For a donor center with many nearby acceptors the total cooperative ET rate is a sum over all acceptor *pairs*. This difference with the first-order ET processes, where the summation is over all single acceptors, causes a different approach to be needed to obtain an analytical formula for dynamics and efficiency.

MONTE CARLO METHOD

In refs 6, 9, and 19 the dynamics of cooperative ET were calculated with a Monte Carlo algorithm. It simulates the distribution of environments, i.e., arrangements of surrounding acceptor ions, that donor ions can have in a crystal where donors and acceptors randomly substitute cation sites. The ordered structure of the crystal allows that the cation sites around a central donor ion are grouped into "shells", i.e., discrete distances at which cation sites can be found (the nearest-neighbor shell, the next-nearest-neighbor shell, etc.). A particular donor environment is characterized by a set of numbers (m_1, m_2, m_3, ...) denoting how many acceptor ions there are in shells (1, 2, 3, ...). This set determines the number of possible acceptor pairs and their separation from the central donor. The total cooperative ET rate of a donor ion with a particular environment is obtained by summing over all acceptor pairs

$$\Gamma_{coop} = C_{coop}\left[\sum_i^{shells} \binom{m_i}{2} r_i^{-12} + \frac{1}{2}\left(\sum_i^{shells} m_i r_i^{-6}\right)^2 - \frac{1}{2}\sum_i^{shells} m_i^2 r_i^{-12}\right] \tag{2}$$

where

$$\binom{m_i}{2} = \frac{m_i!}{m_i!(m_i-2)!}$$

is the binomial coefficient. The first term is for acceptor pairs within the same shell and the other two for acceptor pairs distributed over separate shells (to be precise, the third term cancels same-shell contributions that are contained in the second). The Monte Carlo algorithm randomly generates many environments, accounting for the total number of cation sites (n_1, n_2, n_3, ...) in each of the shells and for the overall acceptor concentration ϕ. Since the ET rate rapidly drops with increasing donor−acceptor separation, it is a good approximation to only take into account a limited number of shells (e.g., only those closer than 1−2 nm). The decay dynamics of the ensemble of donor ions is obtained by adding up the dynamics of all environments simulated

$$I(t) \propto e^{-\Gamma_0 t} \sum_{k=1}^{env.} e^{-\Gamma_{coop}^{(k)} t} \tag{3}$$

where $I(t)$ is the emission intensity at delay time t after the excitation pulse; Γ_0 is the "intrinsic decay rate" of the donors (in the absence of cooperative ET; often the purely radiative decay rate); the summation runs over the environments simulated; and $\Gamma_{coop}^{(k)}$ is the cooperative ET rate for environment k (eq 2). To prove that cooperative ET takes place in a certain donor−acceptor couple, the Monte Carlo model should reproduce the experimental ET dynamics for all acceptor concentrations with a single value for the ET strength C_{coop}.

QUASI-CONTINUOUS MODEL

Here we present a quasi-continuous model that provides an approximate analytical expression for the decay dynamics of cooperative ET in a codoped crystalline material. It has several advantages over the Monte Carlo algorithm described above and previously used in our group. Most importantly, it does not involve Monte Carlo simulations which can be difficult to implement. Second, the expression is shorter (2−13 exponents with fixed relative rates and amplitudes) so that data fitting is faster and easier. And third, it does not require full knowledge of the crystal structure in terms of "shells" as described above.

In the quasi-continuous model only the first shell (i.e., the nearest neighbors) is treated in a discrete way. We explicitly take into account that it contains an integer number of acceptor ions. In contrast, the rate distribution for ET to the crystal environment beyond the first shell (i.e., next-nearest neighbors and further) is averaged out. The probability $A(m_1)$ that a central donor has m_1 nearest-neighbor acceptors in a crystal structure with in total n_1 nearest-neighbor cation sites follows a binomial distribution. It depends on the overall cation concentration ϕ and is given by

$$A(m_1) = \binom{n_1}{m_1} \phi^{m_1} (1-\phi)^{n_1 - m_1} \tag{4}$$

The rate of cooperative ET $\Gamma_{coop}(m_1)$ for a donor ion with m_1 nearest-neighbor acceptors is obtained by summing over all acceptor pairs, each adding a contribution to the total ET rate according to eq 1. Averaging out the ET to acceptors beyond the first shell, we obtain the following expression

$$\Gamma_{coop}(m_1) = C_{coop}\left[\binom{m_1}{2} r_1^{-12} + m_1 \phi r_1^{-6} \Sigma + \frac{\phi^2}{2}\Sigma^2\right] \tag{5}$$

DOI: 10.1021/jp511733g
J. Phys. Chem. C 2015, 119, 2364−2370

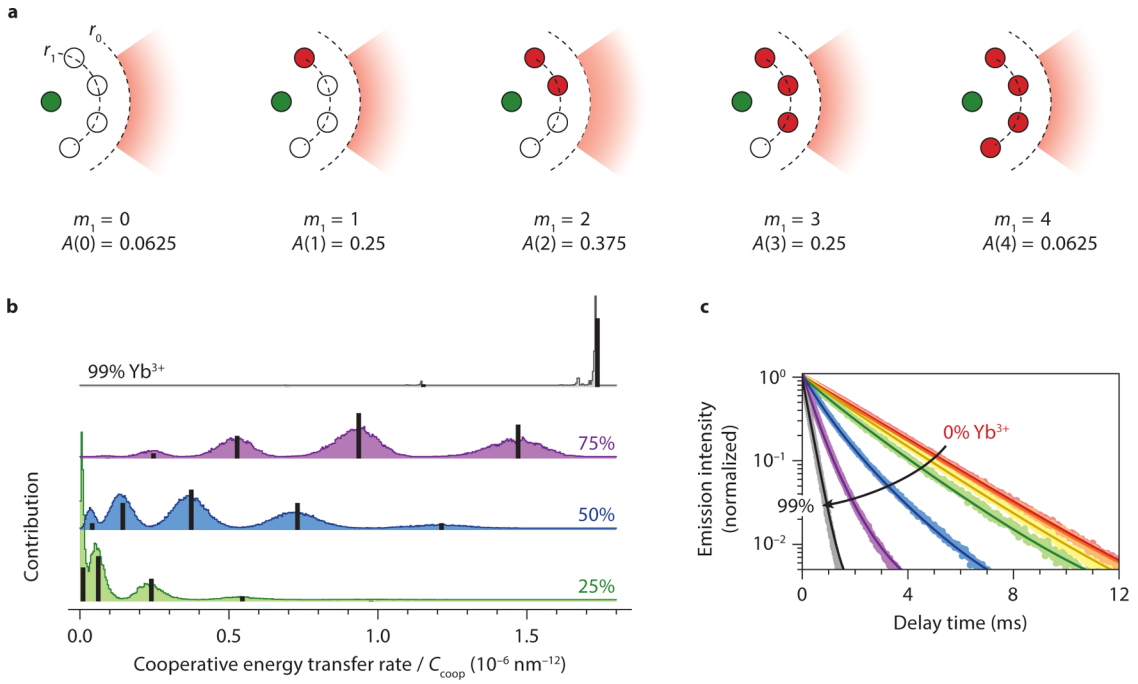

Figure 2. Quasi-continuous (QC) model applied to cooperative ET in YPO_4:Tb^{3+},Yb^{3+}. (a) In the YPO_4 crystal with $n_1 = 4$ nearest-neighbor cation sites, the quasi-continuous model explicitly considers $n_1 + 1 = 5$ different donor environments with $m_1 = 0$, 1, 2, 3, or 4 nearest-neighbor acceptors. The acceptor density beyond the first shell is averaged out to a fixed value of $\rho\phi$. The numbers $A(m_1)$ indicate the probabilities for each of the five environments at an acceptor concentration of $\phi = 50\%$. (b) The distribution of ET rates at different acceptor concentrations (25%, 50%, 75%, 99%). The colored histograms represent the full distributions obtained with a Monte Carlo simulation, while the black bars are the approximation of the quasi-continuous model. (c) The result of fitting the experimental decay dynamics in YPO_4:Tb^{3+}(1%)Yb^{3+}(x%) with x = 0, 5, 15, 25, 50, 75, and 99 to the quasi-continuous model (eq 8). Experimental data are reproduced from ref 6, with excitation in the $^7F_6 \rightarrow {}^5D_4$ transition at 489.6 nm and detection of the $^5D_4 \rightarrow {}^7F_5$ emission at 544 nm. All experimental curves are fitted accurately with a single value for the ET strength of $C_{coop} = 1.99 \times 10^{-6}$ nm^{12} ms^{-1}.

Here the first term in eq 5 represents ET to a pair of nearest-neighbor acceptors, the second term ET with one of the acceptors a nearest-neighbor, and the last term ET to two acceptors beyond the first shell. Σ denotes the total acceptor strength of all cation sites beyond the first shell (i.e., the next-nearest neighbors and further). We can get a simple expression for it by integration

$$\Sigma = \int_{r_0}^{\infty} \rho r^{-6} 4\pi r^2 \mathrm{d}r = \frac{4\pi\rho}{3r_0^3} \tag{6}$$

where ρ is the (average) number density of cation sites in the crystal. r_0 is a cutoff distance that separates the first shell of nearest neighbors from the rest of the crystal and must be chosen somewhere between the nearest-neighbor distance and the next-nearest-neighbor distance. We found that a good definition is

$$r_0^3 = \frac{9n_1}{8\pi\rho} \tag{7}$$

This definition is such that a sphere with radius r_0 contains $1.5n_1$ cations. Conveniently, it does not require knowledge of the exact crystal structure beyond the first shell. We tested that this definition yields a close approximation to the results of the Monte Carlo method for different crystal geometries (see below). The final expression for the decay dynamics of the ensemble of donor ions in the crystal is

$$I(t) = I(0)\mathrm{e}^{-\Gamma_0 t} \sum_{m_1=0}^{n_1} A(m_1)\mathrm{e}^{-\Gamma_{coop}(m_1)t} \tag{8}$$

Hence, for a crystal structure where each cation site has n_1 nearest neighbors, the quasi-continuous model considers $(n_1 + 1)$ different environments (namely, those with $m_1 = 0$, 1, ..., n_1) yielding a model decay function of $(n_1 + 1)$ exponentials. The relative amplitudes and the relative cooperative ET rates are fixed, so that ET is described by a single fit parameter C_{coop} defined as in eq 1.

RESULTS AND DISCUSSION

Cooperative ET in YPO_4:Tb^{3+},Yb^{3+}. As an example, we use the quasi-continuous model to fit the dynamics of Tb^{3+}-to-Yb^{3+} ET in YPO_4, which has previously been shown to be a cooperative process.[6] YPO_4 has a cation density of $\rho = 14.0$ nm^{-3}, with $n_1 = 4$ nearest neighbors surrounding each cation site at a distance of $r_1 = 0.376$ nm. Figure 2a shows the five different donor environments considered by the quasi-continuous model. The first shell can be filled (from left to right) with 0, 1, 2, 3, or 4 nearest neighbors, while the rest of the crystal (beyond cutoff distance r_0) always has an acceptor density of $\rho\phi$. The overall acceptor concentration ϕ is reflected in the probabilities of the five possible environments (given by eq 4). For example, at $\phi = 50\%$ the probabilities $A(m_1)$ of the different environments are as given in Figure 2a, with the most probable environment the one with $m_1 = 2$.

Figure 2b shows the distribution of cooperative ET rates at different acceptor concentrations (from bottom to top: 25%, 50%, 75%, and 99%) in YPO_4. The colored histograms are the distributions obtained from a full Monte Carlo simulation, taking into account all shells in a discrete way. The black bars show how the relative amplitudes (eq 4) and ET rates (eq 5) of

DOI: 10.1021/jp511733g
J. Phys. Chem. C 2015, 119, 2364−2370

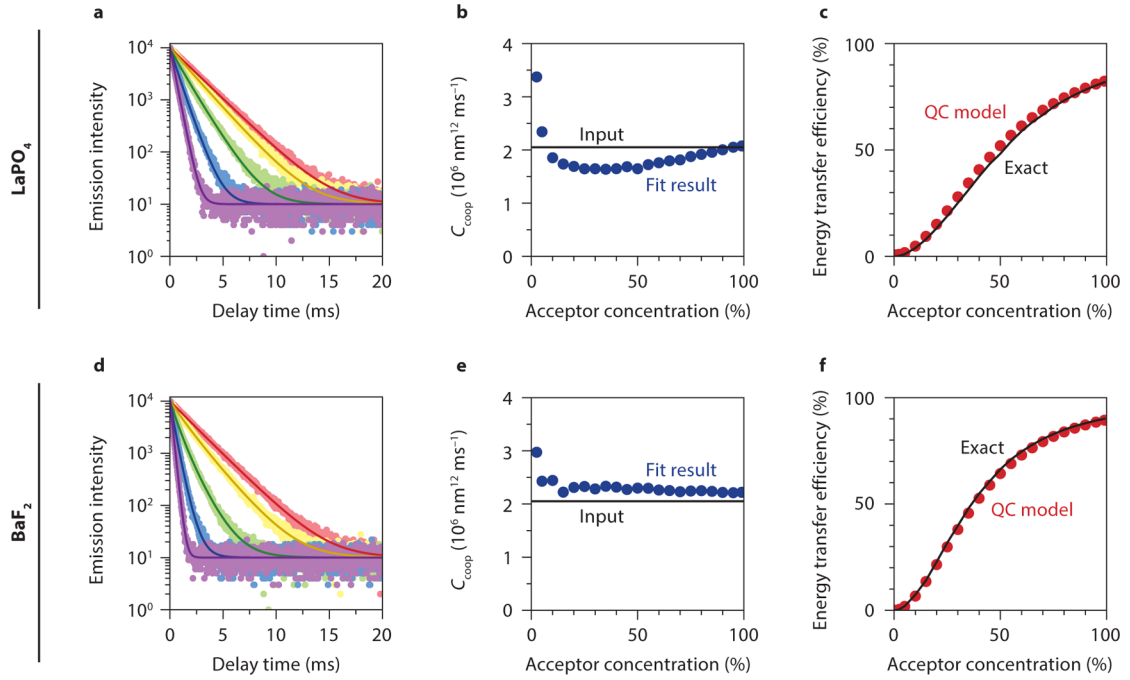

Figure 3. Accuracy of the quasi-continuous (QC) model for cooperative ET, for various acceptor concentrations and different crystal structures. We test how the quasi-continuous model, which takes into account the crystallinity of the host material only for the nearest-neighbor shell, performs for (a,b,c) $LaPO_4$ (monoclinic monazite structure; 2 nearest neighbors at r_1 = 0.410 nm; cation density of ρ = 13.0 nm^{-3}) and (d,e,f) BaF_2 (cubic fluorite structure; 12 nearest neighbors at r_1 = 0.438 nm; cation density of ρ = 16.8 nm^{-3}). (a,d) Simulated PL decay curves (symbols) generated by adding Poissonian noise to the Monte Carlo model for 10 (red), 25 (yellow), 50 (green), 75 (blue), and 99% (purple) acceptor concentration. The input parameters are the crystal structures, Γ_0 = 1/2.30 ms and C_{coop} = 2.05 × 10^{-6} nm^{12} ms^{-1}. Solid lines are fits with the quasi-continuous model. In the fits the intrinsic decay rate is fixed. (b,e) The best-fit values (blue circles) for C_{coop} that the quasi-continuous model extracts from the simulated data. Solid line is the input value for C_{coop}. (c,f) The cooperative ET efficiency according to the expression from the quasi-continuous model (red circles; with input C_{coop} = 2.05 × 10^{-6} nm^{12} ms^{-1}), compared to the ET efficiency from a full Monte Carlo simulation (black solid line).

the quasi-continuous model provide a good approximation of the full distribution.

We take the experimental results of Vergeer et al.[6] and do a global least-squares fit to the model dynamics of eq 8. The result is presented in Figure 2c. With a single value for the ET strength C_{coop} the quasi-continuous model very accurately reproduces the decay dynamics for all acceptor concentrations from 0% to 99% Yb^{3+}. We obtain fitted values of Γ_0 = 1/2.30 ms and C_{coop} = 1.99 × 10^{-6} nm^{12} ms^{-1}. The fitted ET strength lies very close to the C_{coop} = 2.05 × 10^{-6} nm^{12} ms^{-1} obtained from a Monte Carlo fit,[6] demonstrating that the much simpler quasi-continuous model yields a good approximate method to obtain the same results.

Effect of the Crystal Geometry. Since the number of exponents in the quasi-continuous model (eq 8) depends on the crystal geometry, it is important to test that the model works well also for other host crystal structures than YPO_4. In Figure 3 we consider the low-symmetry structure of $LaPO_4$ (panels a,b,c; 2 nearest neighbors at r_1 = 0.410 nm; cation density of ρ = 13.0 nm^{-3}) and the high-symmetry structure of BaF_2 (panels d,e,f; 12 nearest neighbors at r_1 = 0.438 nm; cation density of ρ = 16.8 nm^{-3}). Note that BaF_2 was chosen as an example of a crystal with a large number of nearest neighbors. In practice, lanthanide ions do not substitute randomly (as is assumed here) because of the charge difference between Ba^{2+} and Ln^{3+}.[23] Figures 3a,d show simulated data generated with the Monte Carlo model and with Poissonian noise, for acceptor concentrations of 10, 25, 50, 75, and 99%. As input parameters we used the rate constants of YPO_4:$Tb^{3+}$$Yb^{3+}$: Γ_0 = 1/2.30 ms and C_{coop} = 2.05 × 10^{-6} nm^{12} ms^{-1}. Fits with the quasi-continuous model (solid lines) follow the simulated data very well.

Figure 3b,e compares the best fit value for C_{coop} obtained by fitting the simulated data to the quasi-continuous (blue data points). We see that at all acceptor concentrations >5% and for both crystal structures the fit value obtained is within 25% of the input value (solid line). At the lowest acceptor concentrations of <5% the fits are worse because at such low concentrations ET is weak and its effect on the decay curves obscured by noise. Hence, the cooperative ET strength C_{coop} should always be obtained from a sample with acceptor concentrations >10%. The maximum 25% error introduced by the approximations of the quasi-continuous model in the fitted value of C_{coop} is acceptable in view of the many other sources of uncertainties that are hard to capture in a model. For example, defects in the crystal can act as unintentional acceptors (contributing most strongly at low acceptor concentration). Moreover, the actual distribution of donor and acceptor ions over cation sites may deviate from the random positioning assumed, or energy migration over the donor sublattice can partially average out the statistical distribution of environments. Note that the error becomes much smaller than 25% with a global fit, on measurements of different acceptor concentrations simultaneously.

It is straightforward to calculate the efficiency of cooperative ET for each particular environment in the quasi-continuous model (Figure 2a): $\eta(m_1) = \Gamma_{coop}/(\Gamma_{coop}(m_1) + \Gamma_0)$. To obtain the ensemble averaged efficiency one simply takes the weighted average (which is equivalent to taking the area under the curve described by eq 8)

DOI: 10.1021/jp511733g
J. Phys. Chem. C 2015, 119, 2364−2370

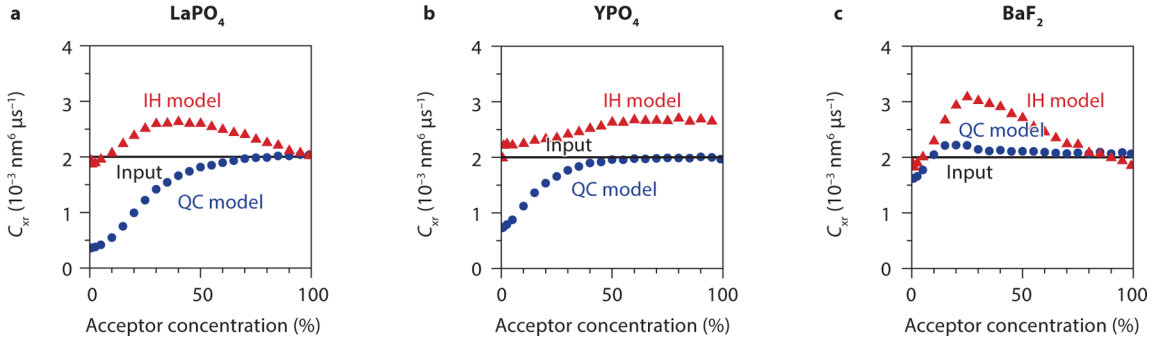

Figure 4. Performance of the quasi-continuous (QC) model in the case of first-order ET. We generate simulated PL decay curves for a cross-relaxation process and use the quasi-continuous model to extract the input parameter of $C_{xr} = 2 \times 10^{-3}$ nm^6 μs^{-1} (with $\Gamma_0 = 1/35$ μs). The quasi-continuous model (blue circles) is compared to the commonly used Inokuti-Hiroyama model (red triangles) for (a) $LaPO_4$ (monoclinic monazite structure; 2 nearest neighbors at $r_1 = 0.410$ nm; cation density of $\rho = 13.0$ nm^{-3}), (b) YPO_4 (tetragonal xenotime structure; 4 nearest neighbors at $r_1 = 0.376$ nm; cation density of $\rho = 14.0$ nm^{-3}), and (c) BaF_2 (cubic fluorite structure; 12 nearest neighbors at $r_1 = 0.438$ nm; cation density of $\rho = 16.8$ nm^{-3}).

$$\eta = \sum_{m_1=0}^{n_1} A(m_1) \frac{\Gamma_{coop}(m_1)}{\Gamma_{coop}(m_1) + \Gamma_0} \tag{9}$$

where $A(m_1)$ and $\Gamma_{coop}(m_1)$ are given by eqs 4 and 5, respectively. Figure 3c,f shows that this formula for the cooperative ET efficiency (red circles) accurately reproduces the efficiency calculated with a Monte Carlo simulation (solid black lines), for both crystal geometries and for all acceptor concentrations.

Beyond Cooperative ET. We have now demonstrated that the quasi-continuous model can accurately reproduce and fit the dynamics of cooperative ET. Next, we discuss how the model can be further extended. For example, if one wishes to use a quasi-continuous model for the first-order ET process of cross-relaxation[9,15,16] (xr; rate of ET by dipole−dipole coupling per donor−acceptor pair $\propto r_{DA}^{-6}$), the expression for the ET rate of a donor with m_1 nearest neighbors becomes

$$\Gamma_{xr} = C_{xr}[m_1 r_1^{-6} + \phi\Sigma] \tag{10}$$

and the decay dynamics of the ensemble of donor ions are given by

$$I(t) = I(0)e^{-\Gamma_0 t} \sum_{m_1=0}^{n_1} A(m_1) e^{-\Gamma_{xr}(m_1)t} \tag{11}$$

We have tested this expression, again by fitting to data generated with a Monte Carlo model (realistic input parameters as in $LiYF_4$:Pr^{3+},Yb^{3+}:[9] $\Gamma_0 = 1/35$ μs; $C_{xr} = 2 \times 10^{-3}$ nm^6 μs^{-1}). Figure 4 compares the cross-relaxation ET strength C_{xr} fitted with the quasi-continuous model (blue cirles) to the input (black solid line), as well as the values obtained with the commonly used model of Inokuti and Hiroyama[21] (red triangles), in order of increasing symmetry for $LaPO_4$ (Figure 4a), for YPO_4 (Figure 4b), and for BaF_2 (Figure 4c). There is a trend that the quasi-continuous model is better (i.e., finds a value for C_{xr} closer to the input value) at a higher number of nearest neighbors, as expected since the model treats the nearest neighbors exactly. Nevertheless, we see that our model finds the input value for C_{xr} within 10% at high acceptor concentrations >30% for all crystal structures. At low concentrations (<20%) the quasi-continuous model can be off by >50% depending on crystal structure and acceptor concentration. The biggest deviations with the input value occur in the limit of low acceptor concentrations and a small number of nearest neighbors (e.g., in $LaPO_4$; Figure 4a). This can be understood by realizing that in this limit the expression provided by the quasi-continuous model (eq 10) is dominated by a single term (namely, the one for zero nearest-neighbor acceptors), while the many possible acceptor distributions beyond the nearest-neighbor shell are not explicitly taken into account. We see, however, that also the commonly used Inokuti-Hiroyama model is off by more than 25% in many cases. Hence, the exact analytical expression[19,20] is preferrable over both the quasi-continuous and the Inokuti-Hiroyama models to accurately fit first-order ET dynamics. Only at low acceptor concentrations (<10%) the Inokuti-Hiroyama is a good approximation, while in high-symmetry crystals or at high acceptor concentrations (>30%) the quasi-contious model performs better.

The quasi-continuous model can very conveniently be used to model a combination of different ET mechanisms. For example, a combination of cooperative ET and cross-relaxation would yield decay dynamics given by

$$I(t) = I(0)e^{-\Gamma_0 t} \sum_{m_1=0}^{n_1} A(m_1) e^{-[\Gamma_{coop}(m_1)+\Gamma_{xr}(m_1)]t} \tag{12}$$

Such a model could be used to determine the relative contributions of cross-relaxation and cooperative to the ET for a particular donor−acceptor couple, by fitting the parameters C_{coop} and C_{xr}. Several other extensions to the quasi-continuous model are thinkable. For example, one could adjust eqs 8 and 11 to describe ET mechanisms with another distance dependence than $\propto r^{-6}$ as for dipole−dipole interaction (such as $\propto r^{-8}$ for dipole−quadrupole interaction or $\exp(-r/d)$ for exchange interaction) or even use Σ as a free fit parameter to determine the range of the interaction from a fit. Moreover, it possible to improve the accuracy of the model further (at the cost of increased complexity) by also explicitly considering the possible acceptor distributions in the next-nearest-neighbor shell, rather than only the nearest-neighbor shell. This addition can be especially useful for crystal lattices with a small number of nearest neighbors.

CONCLUSION

To summarize, we have presented a simple analytical model for cooperative ET in codoped crystals. The model explicitly takes into account the possible nearest-neighbor environments of the

DOI: 10.1021/jp511733g
J. Phys. Chem. C 2015, 119, 2364−2370

energy donor ion but averages out the effect of the rest of the crystal. The result is a multiexponential model function for the ET dynamics with relative amplitudes and decay constants fixed (depending on the concentration of acceptor ions) that can directly be used to fit experimental data. The model works well for cooperative ET in $YPO_4:Tb^{3+},Yb^{3+}$,[6] excellently reproducing the experimental trends and yielding a very similar value for the ET strength C_{coop} as obtained from a more involved Monte Carlo algorithm. The accuracy of the model is good for various crystal host geometries, as confirmed by its power at extracting the input parameters from simulated data. We also investigate the applicability of the quasi-continuous model to first-order ET processes by dipole−dipole interaction, such as cross-relaxation. For high-symmetry crystals or at acceptor concentrations >30% it is more accurate than the commonly used Inokuti-Hiroyama model. Our simple model provides a convenient method to identify the ET processes operative in codoped crystals and quantify ET rates and efficiencies.

AUTHOR INFORMATION

Corresponding Author

*E-mail: a.meijerink@uu.nl.

Notes

The authors declare no competing financial interest.

REFERENCES

(1) Zhou, J.; Liu, Z.; Li, F. Upconversion Nanophosphors for Small-Animal Imaging. *Chem. Soc. Rev.* **2011**, *41*, 1323−1349.

(2) Erickson, C. S.; Bradshaw, L. R.; McDowall, S.; Gilbertson, J. D.; Gamelin, D. R.; Patrick, D. L. Zero-Reabsorption Doped-Nanocrystal Luminescent Solar Concentrators. *ACS Nano* **2014**, *8*, 3461−3467.

(3) Wegh, R. T.; Donker, H.; Oskam, K. D.; Meijerink, A. Visible Quantum Cutting in $LiGdF_4:Eu^{3+}$ through Downconversion. *Science* **1999**, *283*, 663−666.

(4) Van der Ende, B. M.; Aarts, L.; Meijerink, A. Lanthanide Ions as Spectral Converters for Solar Cells. *Phys. Chem. Chem. Phys.* **2009**, *11*, 11081−11095.

(5) Zhang, Q. Y.; Huang, X. Y. Recent Progress in Quantum Cutting Phosphors. *Prog. Mater. Sci.* **2010**, *55*, 353−427.

(6) Vergeer, P.; Vlugt, T. J. H.; Kox, M. H. F.; Den Hertog, M. I.; Van der Eerden, J. P. J. M.; Meijerink, A. Quantum Cutting by Cooperative Energy Transfer in $Yb_xY_{1-x}PO_4:Tb^{3+}$. *Phys. Rev. B* **2005**, *71*, 014119.

(7) Feldmann, C.; Jüstel, T.; Ronda, C. R.; Wiechert, D. U. Quantum Efficiency of Down-Conversion Phosphor $LiGdF_4:Eu$. *J. Lumin.* **2001**, *92*, 245−254.

(8) Tzeng, H.-Y.; Cheng, B.-M.; Chen, T.-M. Visible Quantum Cutting in Green-Emitting $BaGdF_5:Tb^{3+}$ Phosphors via Down-conversion. *J. Lumin.* **2007**, *122−123*, 917−920.

(9) Van Wijngaarden, T.; Scheidelaar, S.; Vlugt, T. J. H.; Reid, M. F.; Meijerink, A. Energy Transfer Mechanism for Downconversion in the (Pr^{3+}, Yb^{3+}) Couple. *Phys. Rev. B* **2010**, *81*, 155112.

(10) Deng, K.; Gong, T.; Hu, L.; Wei, X.; Chen, Y.; Yin, M. Efficient Near-Infrared Quantum Cutting in $NaYF_4:Ho^{3+},Yb^{3+}$ for Solar Photovoltaics. *Opt. Express* **2011**, *19*, 1749−1754.

(11) Zhang, Q. Y.; Yang, C. H.; Pan, Y. X. Cooperative Quantum Cutting in One-Dimensional $(Yb_xGd_{1-x})Al_3(BO_3)_4:Tb^{3+}$ Nanorods. *Appl. Phys. Lett.* **2007**, *90*, 021107.

(12) Chen, D. Q.; Wang, Y. S.; Yu, Y. L.; Huang, P.; Weng, F. Y. Near-Infrared Quantum Cutting in Transparent Nanostructured Glass Ceramics. *Opt. Lett.* **2008**, *33*, 1884−1886.

(13) Ueda, J.; Tanabe, S. Visible to Near Infrared Conversion in Ce^{3+}−Yb^{3+} Co-Doped YAG Ceramics. *J. Appl. Phys.* **2009**, *106*, 043101.

(14) Xie, L.; Wang, Y.; Zhang, H. Near-Infrared Quantum Cutting in $YPO_4:Yb^{3+},Tm^{3+}$ *via* Cooperative Energy Transfer. *Appl. Phys. Lett.* **2009**, *94*, 061905.

(15) Eilers, J. J.; Biner, D.; Van Wijngaarden, J. T.; Krämer, K.; Güdel, H.-U.; Meijerink, A. Efficient Visible to Infrared Quantum Cutting through Downconversion with the Er^{3+}-Yb^{3+} couple in $Cs_3Y_2Br_9$. *Appl. Phys. Lett.* **2010**, *96*, 151106.

(16) Zheng, W.; Zhu, H.; Li, R.; Tu, D.; Liu, Y.; Luo, W.; Chen, X. Visible-to-Infrared Quantum Cutting by Phonon-Assisted Energy Transfer in $YPO_4:Tm^{3+},Yb^{3+}$ Phosphors. *Phys. Chem. Chem. Phys.* **2012**, *14*, 6974−6980.

(17) Liu, T.-C.; Zhang, G.; Qiao, X.; Wang, J.; Seo, H. J.; Tsai, D.-P.; Liu, R.-S. Near-Infrared Quantum Cutting Platform in Thermally Stable Phosphate Phosphors for Solar Cells. *Inorg. Chem.* **2013**, *52*, 7352−7357.

(18) Timmerman, D.; Valenta, J.; Dohnalová, K.; De Boer, W. D. A. M.; Gregorkiewicz, T. Step-like Enhancement of Luminescence Quantum Yield of Silicon Nanocrystals. *Nat. Nanotechnol.* **2011**, *6*, 710−713.

(19) Yu, D. C.; Rabouw, F. T.; Boon, W. Q.; Kieboom, T.; Ye, S.; Zhang, Q. Y.; Meijerink, A. Insights into the Energy Transfer Mechanism in Ce^{3+}-Yb^{3+} Codoped YAG Phosphors. *Phys. Rev. B* **2014**, *90*, 165126.

(20) Rabouw, F. T.; Den Hartog, S. A.; Senden, T.; Meijerink, A. Photonic Effects on the Förster Resonance Energy Transfer Efficiency. *Nat. Commun.* **2014**, *5*, 3610.

(21) Inokuti, M.; Hirayama, F. Influence of Energy Transfer by the Exchange Mechanism on Donor Luminescence. *J. Chem. Phys.* **1965**, *43*, 1978−1989.

(22) Yokota, M.; Tanimoto, O. Effects of Diffusion on Energy Transfer by Resonance. *J. Phys. Soc. Jpn.* **1967**, *22*, 779−784.

(23) Miller, M. P.; Wright, J. C. Single Site Multiphonon and Energy Transfer Relaxation Phenomena in $BaF_2:Er^{3+}$. *J. Chem. Phys.* **1978**, *68*, 1548−1562.

DOI: 10.1021/jp511733g
J. Phys. Chem. C 2015, 119, 2364−2370